



VICTORIA UNIVERSITY
MELBOURNE AUSTRALIA

Development and characterisation of HPMC films containing PLA nanoparticles loaded with green tea extract for food packaging applications

This is the Accepted version of the following publication

Wrona, M, Cran, Marlene, Nerín, C and Bigger, Stephen W (2017)
Development and characterisation of HPMC films containing PLA
nanoparticles loaded with green tea extract for food packaging applications.
Carbohydrate Polymers, 156. 108 - 117. ISSN 0144-8617

The publisher's official version can be found at
<http://www.sciencedirect.com/science/article/pii/S0144861716310475>
Note that access to this version may require subscription.

Downloaded from VU Research Repository <https://vuir.vu.edu.au/33826/>

1 **Development and Characterisation of HPMC Films Containing**
2 **PLA Nanoparticles Loaded with Green Tea Extract for Food**
3 **Packaging Applications**

5 Magdalena Wrona^a, Marlene J. Cran^{b*}, Cristina Nerín^a and Stephen W. Bigger^b.

6 ^a Department of Analytical Chemistry, Aragon Institute of Engineering Research
7 I3A, CPS-University of Zaragoza, Torres Quevedo Building, María de Luna St.
8 3, E-50018 Zaragoza, Spain

9 ^b Institute for Sustainability and Innovation, Victoria University, PO Box 14428,
10 Melbourne, 8001, Australia

11 *Corresponding author: Tel.: + 61 3 9919 7642; fax: +61 3 9919 8082

12 E-mail addresses: marlene.cran@vu.edu.au (M.J. Cran),
13 magdalenka.wrona@gmail.com (M. Wrona), cnerin@unizar.es (C. Nerín),
14 stephen.bigger@vu.edu.au (S.W. Bigger)

15

16 **Abstract**

17 A novel active film material based on hydroxypropyl-methylcellulose
18 (HPMC) containing poly(lactic acid) (PLA) nanoparticles (NPs) loaded with
19 antioxidant (AO) green tea extract (GTE) was successfully developed. The PLA
20 NPs were fabricated using an emulsification-solvent evaporation technique and
21 the sizes were varied to enable a controlled release of the AO from the HPMC
22 matrix. A statistical experimental design was used to optimize the synthesis of
23 the NPs in order to obtain different sizes of nanoparticles and the loading of these
24 into the HPMC matrix was also varied. The physico-chemical properties of the
25 composite films were investigated and the release of the AO was confirmed by
26 migration studies in 50% v/v ethanol/water food simulant. The AO capacity of the
27 GTE released from the active films was studied using the 2,2-diphenyl-1-
28 picrylhydrazyl (DPPH) radical method and the results suggest that the material
29 could potentially be used for extending the shelf-life of food products with high fat
30 content.

31

32 **Keywords:** green tea extract, antioxidants, PLA, nanoparticles, HPMC, active
33 packaging

34

35 **1 Introduction**

36 In the broad field of nanotechnology, nanocomposites based on polymer
37 matrices have become a very popular topic. Polymer nanocomposites are
38 considered a major technological breakthrough for many engineering
39 applications. For example, carbon nanotubes can deliver exceptional mechanical
40 properties to a range of polymer matrices. Nanoparticles incorporated into
41 polymers can enhance their barrier properties as well as their chemical and
42 electrical properties, and can also impart reinforcement to polymer matrices (Ma,
43 Siddiqui, Marom & Kim, 2010; Paul & Robeson, 2008; Ruffino, Torrisi, Marletta &
44 Grimaldi, 2011).

45 Considerable attention has emerged over recent years towards the
46 development of hybrid materials for active packaging applications. Combining the
47 characteristics of organic polymers and nanotechnology innovations has led to
48 the creation of new materials with extraordinary properties (Cirillo, Spizzirri &
49 Iemma, 2015; Cushen, Kerry, Morris, Cruz-Romero & Cummins, 2012; Duncan,
50 2011; Rhim, Park & Ha, 2013; Silvestre, Duraccio & Cimmino, 2011). In particular,
51 newly developed biopolymers that degrade under natural composting conditions
52 combined with antioxidant (AO) and antimicrobial (AM) properties are becoming
53 increasingly popular (DeGruson, 2016; Fabra, López-Rubio & Lagaron, 2014).
54 These materials are the result of consumer demands for fresh foods with
55 extended shelf life as well as natural packaging materials with a reduced
56 environmental footprint.

57 One such biopolymer is poly(lactic acid) (PLA), an aliphatic polyester whose
58 monomer can be derived primarily from renewable agricultural resources such as
59 corn, beetroot, and sugarcane. The polymer is formed *via* the fermentation of
60 starch and condensation of lactic acid (Bang & Kim, 2012; Del Nobile, Conte,
61 Buonocore, Incoronato, Massaro & Panza, 2009; Llana-Ruiz-Cabello et al., 2015;
62 Rancan et al., 2009; Tawakkal, Cran, Miltz & Bigger, 2014). Although it is typically
63 produced for primary packaging applications, PLA can also be further processed
64 to form nanoparticles (Hirsjärvi, 2008; Rancan et al., 2009; Ruan & Feng, 2003).

65 Nanoparticles are commonly defined as particles with one or more
66 dimensions in the range between 10 to 1000 nm (Rao & Geckeler, 2011). In terms
67 of nanocarriers for the delivery or encapsulation of additives, they can be
68 generally categorised into two groups: nanocapsules and nanospheres. The
69 former are nanocarriers where an active agent is presented in a liquid core
70 surrounded by a polymer shell whereas the latter are nanocarriers where the
71 active agent is encapsulated inside the polymer or adsorbed on the surface of
72 the polymer (Fang & Bhandari, 2010; Rao & Geckeler, 2011). Extensive studies
73 have been conducted in applying PLA nanoparticles to the development of new
74 types of active packaging (Auras, Harte & Selke, 2004; Imran, Klouj, Revol-
75 Junelles & Desobry, 2014; Roussaki et al., 2014; Samsudin, Soto-Valdez &
76 Auras, 2014). Such nanoparticles offer opportunities to protect active molecules
77 against degradation during the manufacturing of materials that can often involve
78 thermooxidative processes.

79 The main goals in the design of nanoparticles for AO delivery in active
80 packaging are the control of nanoparticle size, loading and release of the AO,
81 and the surface properties (Armentano et al., 2013). The emulsification-solvent

82 evaporation technique is a physico-chemical method of encapsulation where the
83 solvent enables the partial or complete dissolution of the polymer and the
84 emulsifier enables size control as well as enhancing the drug or AO solubility in
85 the polymer network. In this technique, the loading of active agents occurs by
86 entrapment and polymeric nanoparticles can be successfully used for
87 encapsulation of both lipophilic and hydrophilic active agents (Gao, Jones, Chen,
88 Liang, Prud'homme & Leroux, 2008; Vrignaud, Benoit & Saulnier, 2011). The
89 encapsulation of AOs can be influenced by factors such as the molecular weight
90 of the agent, its predisposition to interaction with the polymer matrix, and the
91 presence of specific functional groups in the AO structure (Armentano et al.,
92 2013).

93 Semi-synthetic materials derived from cellulose such as hydroxypropyl-
94 methylcellulose (HPMC) have been used successfully to develop a range of
95 active packaging materials (Akhtar, Jacquot, Arab-Tehrany, Gaiani, Linder &
96 Desobry, 2010; Bilbao-Sainz, Avena-Bustillos, Wood, Williams & McHugh, 2010;
97 Brindle & Krochta, 2008; de Moura, Aouada, Avena-Bustillos, McHugh, Krochta
98 & Mattoso, 2009; de Moura, Avena-Bustillos, McHugh, Krochta & Mattoso, 2008;
99 Ding, Zhang & Li, 2015; Imran, Klouj, Revol-Junelles & Desobry, 2014).
100 Packaging films derived from HPMC have low flavour and aroma properties,
101 which is important in food applications (Akhtar et al., 2012; Sanchez-Gonzalez,
102 Vargas, Gonzalez-Martinez, Chiralt & Chafer, 2009), and the polymer is approved
103 by the European Commission (2011) as a food additive characterised by number
104 E 464.

105 Lipid oxidation is the main cause of fatty food spoilage (Falowo, Fayemi &
106 Muchenje, 2014; Min & Ahn, 2005) and there is a significant number of

107 publications describing developments in active packaging designed to improve
108 food products containing high levels of polyunsaturated fatty acids (Bolumar,
109 Andersen & Orlien, 2011; Camo, Lorés, Djenane, Beltrán & Roncalés, 2011;
110 López-de-Dicastillo, Gómez-Estaca, Catalá, Gavara & Hernández-Muñoz, 2012);
111 Nerin et al 2006; Carrizo et al 2016). These are primarily focused on AO
112 compounds such as green tea or green tea extracts (s) that have been
113 successfully used to protect against lipid oxidation (Carrizo, Gullo, Bosetti &
114 Nerín, 2014; Frankel, Huang & Aeschbach, 1997; Yang, Lee, Won & Song, 2016;
115 Yin, Becker, Andersen & Skibsted, 2012). The main compounds in green tea are
116 catechins that are powerful AOs due to the presence of the phenolic hydroxyl
117 groups in their structure (Colon & Nerin, 2012; Gadkari & Balaraman, 2015;
118 Senanayake, 2013). For direct contact applications, the AO agent would typically
119 not be required to be released over time in order to extend the shelf-life of
120 products (Carrizo, Taborda, Nerín & Bosetti, 2016), however, encapsulation of
121 the agents can further extend the applications to releasing systems.

122 Active packaging using AO compounds faces several challenges including
123 the protection of AOs during the production of packaging materials and the
124 controlled release of encapsulated AOs from the polymer matrix. The present
125 work aims to address these challenges with the development of a new hybrid
126 active film based on natural AOs incorporated into a HPMC biopolymer film. This
127 paper reports the synthesis and characterisation of GTE-loaded PLA
128 nanoparticles of various sizes incorporated into a HPMC film matrix to achieve
129 controlled AO release.

130
131 **2 Materials and Methods**

132 **2.1 Polymers and Reagents**

133 The PLA polymer (grade 7001D IngeoTM, specific gravity 1.24, melting
134 temperature 154°C (Tawakkal, Cran & Bigger, 2014), was provided in pellet form
135 by NatureWorks LLC, Minnetonka, Minnesota, USA. The HPMC powder
136 (viscosity at 2% w/w in H₂O of 80-120 cP; CAS 9004-65-3), poly(vinyl alcohol)
137 (PVA) (99+% hydrolyzed; CAS 9002-89-5) and 2,2-diphenyl-1-picrylhydrazyl
138 (DPPH) radical (CAS 1898-664) were obtained from Sigma-Aldrich (Sydney,
139 Australia). Other chemicals included: acetone (CAS 67-64-1) obtained from
140 Univar (Ingleburn, Australia), acetonitrile (CAS 75-05-8) obtained from Merck
141 (Bayswater, Australia), and methanol (ACS/HPLC; CAS 67-56-1) obtained from
142 Honeywell Burdick and Jackson[®] (Adelaide, Australia). Green tea powder
143 (Asahina Maccha 4-GO) was manufactured by Marushichi Suzuki Shoten Co.
144 and was purchased from a local supermarket. Green tea was stored in darkness
145 at 4°C. Ultrapure water was supplied from a Milli-Q system (Millipore, Billerica,
146 MA, USA).

147

148 **2.2 Green Tea Extract**

149 Green tea extract was prepared by adding 0.5 g of green tea powder to
150 10 mL of an acetonitrile in water solution (4:1 v/v ratio). The solution was heated
151 to 80°C and stirred continuously for 30 min before it was cooled to room
152 temperature and filtered once through filter paper (Whatman 5A, 125 mm from
153 Adventec[®], Caringbah, Australia) and then through a 0.2 µm PHENEX PTFE
154 syringe filter (also from Adventec[®]). Solutions of GTE at a concentration of 1%
155 v/v in acetonitrile were prepared.

156

157 **2.3 Nanoparticle Synthesis**

158 A slightly modified method to that described by Roussaki et al. (2014) was
159 used to produce PLA nanoparticles loaded with GTE with optimization of the
160 synthesis parameters outlined below. Briefly, 20 mL of a 1% v/v aqueous solution
161 of PVA was added to a 250 mL round-bottom flask and the solution was mixed
162 at 700 to 1400 rpm using an egg-shaped magnetic stirrer. A mass of 0.2 g of PLA,
163 which had been previously dried at 60°C in an air-circulating oven overnight, was
164 dissolved in 20 g of acetone at room temperature. Equal volumes (20 mL) of
165 different concentrations (0.2%, 0.6%, 1%) of GTE in acetonitrile and 1% w/v PLA
166 in acetone were mixed and this solution was then added drop-wise into the PVA
167 emulsifier solution where it remained under stirring for 10 min. Samples were left
168 overnight to evaporate the solvent and were then centrifuged at 4000 rpm for 10
169 min at 15°C using a SORVALL® RT7 bench-top centrifuge from Du Pont
170 Company (Wilmington, USA). The nanoparticles suspended in the aqueous
171 phase were thereafter subjected to several cleaning steps by addition of
172 acetonitrile and centrifugation and the resulting supernatant was recovered and
173 stored at 7°C. Two types of GTE-loaded nanoparticles were prepared: (i)
174 emulsifier free at a stirring speed of 1400 rpm, and (ii) in 0.5% v/v PVA emulsifier
175 solution at a stirring speed of 700 rpm. The samples were nominally characterised
176 by small nanoparticles (NP47) and larger nanoparticles (NP117) where the
177 number is the nanoparticle size in nm. Neat nanoparticles without GTE (BK244),
178 were also prepared under the same conditions.

179 The yield of the nanoparticles was determined gravimetrically by weighing
180 a sample of the solution that was then completely dried in an air-circulating oven.
181 After cooling, the residual mass was reweighed and the yield of the nanoparticles
182 calculated based on the mass of the original sample solution. Nanoparticle size

183 optimization was achieved using the computer-aided experimental design
184 software program MODDE 6.0 from Umetrics (Umeå, Sweden). Details of the
185 optimization experimental design are presented in the supplement.

186

187 **2.4 Film Fabrication**

188 A dispersion technique commonly referred to as the "hot/cold" technique
189 proposed by the Dow Chemical Company (2002) was used for HPMC film
190 preparation. Briefly, 6 g of HPMC powder was dissolved in 20 mL of hot water
191 (ca. 90°C) under continuous stirring. When the HPMC powder was dissolved, 40
192 mL of cold water was added and the solution was mixed for a further 30 min
193 without heating. Different amounts of NP47 or NP117 GTE-loaded nanoparticle
194 solutions, i.e. 30 or 60% w/w, were used to prepare the film solutions and the final
195 concentration of dry nanoparticles in the films was 15% and 30% w/w
196 respectively. The films were named based on the size and loading of the
197 nanoparticles, i.e. NP47-15, NP47-30, NP117-15, and NP117-30. Two series of
198 HPMC film solutions with nanoparticles that did not contain GTE, i.e. BK244-15
199 and BK244-30, were also prepared as control films along with neat HPMC film
200 without nanoparticles.

201 Films were prepared by casting that was performed by pipetting a
202 predetermined volume (ca. 6 mL) of solution onto rimmed glass plates (225 cm²)
203 that were then placed on a smooth, level granite slab. The solution was spread
204 evenly with a glass rod and allowed to dry overnight at room temperature to obtain
205 film samples of ca. 20 µm thickness. The actual thickness of each of the films
206 was measured using a hand-held micrometer (Mitutoyo, Japan) with a precision
207 of 0.005 mm and an average of three measurements was taken for each film.

208

209 **2.5 Nanoparticle and Film Characterization**

210 **2.5.1 Nanoparticle Size and Charge**

211 A ca. 2% w/v solution of nanoparticles in DI water was prepared in order
212 to the measure size and surface charge of the nanoparticles. For particle size
213 and polydispersity index (PDI) measurements, 12 mm square polystyrene
214 cuvettes were used whereas disposable, folded capillary zeta cells were used for
215 surface charge measurements. All samples were tested at $25.0 \pm 0.1^\circ\text{C}$ using a
216 Zetasizer Nano ZS instrument from Malvern Instruments (Tarent Point, Australia)
217 equipped with a He–Ne laser source ($\lambda = 633$ nm) with a scattering angle of 173° .
218 The following sample settings were applied: refractive index: 1.330; viscosity:
219 1.000; dispersant: water; equilibration time: 2 min. Dynamic light scattering (DLS)
220 was used to measure particle size; electrophoretic light scattering (ELS) was
221 used for the measurement of particle surface charge; and the PDI was calculated
222 using the cumulant method (Frisken, 2001; Lim, Yeap, Che & Low, 2013). All
223 measurements were performed in triplicate.

224

225 **2.5.2 Film Colour Measurement**

226 A portable Chroma Meter CR-300 from Konika Minolta (Tokyo, Japan) with
227 illuminant D65 and a 2° standard observer was used for the measurement of film
228 colour. An 8 mm diameter measuring head area was used with diffuse illumination
229 and 0° viewing angle, and a white chromameter standard plate ($L = 97.47$, $a =$
230 0.13 , $b = 1.83$) was used for calibration. Sections of each film sample were placed
231 on the standard plate to perform the measurements that were conducted at $25 \pm$
232 1°C and in triplicate. The colour was determined using CIE $L^*a^*b^*$ colour space

233 where L^* represents white ($L^* = 100$) and black ($L^* = 0$) opponent colours,
234 positive/negative values of a^* represent red/green opponent colours respectively,
235 and positive/negative values of b^* represent yellow/blue opponent colours
236 respectively. Equations described by Yam and Papadakis (2004) were used to
237 transform L, a, b values into L^*, a^*, b^* values.

238

239 **2.5.3 Differential Scanning Calorimetry**

240 The melting temperature (T_m), melting enthalpy (ΔH_m) and degree of
241 crystallinity (X_c) of PLA nanoparticles and samples of the HPMC films containing
242 PLA nanoparticles were determined by differential scanning calorimetry (DSC)
243 using a Mettler-Toledo (Greifensee, Switzerland) DSC equipped with STARe
244 Software (version 11.00) for data acquisition and analysis. Samples of ca. 5 mg
245 were weighed and encapsulated in aluminium pans, and an empty aluminium pan
246 (40 μL) was used as the reference. A single dynamic segment was applied over
247 the temperature range of 50-200°C at a heating rate of 10°C min⁻¹. The samples
248 were kept under a 50 mL min⁻¹ nitrogen gas flow during the analysis and single
249 experiments were performed.

250

251 **2.5.4 Fourier-transform Infrared Analysis**

252 Fourier-transform infrared (FTIR) analysis was performed using a Perkin
253 Elmer Frontier™ FTIR spectrophotometer (Waltham, USA) in attenuated total
254 reflectance (ATR) mode using a diamond ATR crystal. The spectra of the
255 nanoparticles, film samples, and neat green tea powder were recorded using 16
256 scans at a resolution of 2 cm⁻¹ over the full mid-IR range (4000–600 cm⁻¹). Data

257 acquisition and analysis were performed using the Perkin Elmer Spectrum
258 software. All measurements were performed in triplicate and at $25 \pm 1^\circ\text{C}$.

259

260 **2.5.5 Scanning Electron Microscopy**

261 High-magnification images of nanoparticles and films were obtained using
262 a scanning electron microscope (SEM). A drop of nanoparticle solution was
263 deposited on an aluminium sample holder covered by double-sided conductive
264 tape and all samples were left to dry. In the case of HPMC film samples, small
265 pieces (ca. 3×3 mm) were cut and also deposited on an aluminium sample
266 holder using conductive tape. All samples were subsequently sputter-coated with
267 iridium using a Polaron SC5750 sputter coater (Quorum Technologies, Laughton,
268 UK). The surface morphology of the nanoparticles and films was observed at 3 kV
269 using a ZEISS Merlin Gemini 2 Field Emission SEM (ZEISS International,
270 Oberkochen, Germany) in high-resolution column mode with images recorded at
271 magnifications of up to 25,000 \times .

272

273 **2.6 Green Tea Migration**

274 Release studies were performed to determine the migration of GTE from
275 the HPMC films into 50% v/v ethanol in water, a lipophilic food simulant, at 20 $^\circ\text{C}$
276 and 40 $^\circ\text{C}$ after 10 days. Double-sided total immersion migration tests were
277 performed by placing 2 \times 3 cm pieces of film in glass vials that were filled with 18
278 mL of the simulant. The absorbance of the samples was measured at 268 nm
279 using a Hach DR 5000TM UV-visible spectrophotometer (Hach Australia, Notting
280 Hill, Victoria, Australia). The spectrophotometric measurements were made
281 against a blank comprised of the ethanol food simulant. The calibration curve of

282 GTE was determined by preparing standard solutions of GTE over the
283 concentration range of 0.04% and 0.60% w/w prepared in 50% v/v ethanol in
284 water. All samples were prepared in triplicate.

285

286 **2.7 Film Antioxidant Capacity**

287 The AO capacity (CAOX) of the GTE released from the active films and of
288 the blank films was determined by the DPPH method (Pyrzynska & Pękal, 2013)
289 using the solutions from the GTE migration test. For this test, five different
290 dilutions of film extracts in methanol were prepared. The reaction was triggered
291 by adding 100 µL of each extract dilution to 3.5 mL of a 30 µg g⁻¹ solution of
292 DPPH in methanol. A blank solution of DPPH in methanol was also prepared and
293 all samples were stored for 15 min in darkness prior to measuring the absorbance
294 of the samples at 515 nm with the same spectrophotometer used in the GTE
295 migration test. The spectrophotometric measurements were performed against a
296 methanol blank and an additional calibration to check the DPPH concentration
297 was also performed. For this purpose, standard solutions of DPPH at
298 concentrations between 5 and 50 µg g⁻¹ were prepared in methanol.

299 The AO capacity of the samples was expressed as the percentage of
300 inhibition of DPPH (%) that was calculated according to following formula:

301

302
$$\text{I\%} = [(A_0 - A)/A_0] \times 100$$

303

304 where A_0 and A are the absorbance values of the blank (DPPH in methanol) and
305 the extract sample (DPPH with extract) respectively. The value of I% after 15 min
306 was plotted against the concentration of the AO and a linear regression analysis

307 was performed to obtain the half maximal inhibitory concentration (IC_{50}) value
308 which is inversely proportional to the AO capacity (Pyrzynska & Pękal, 2013).
309 The results are represented as a percentage of the liberated substance.

310

311 **2.8 Statistical Analysis**

312 A Student t test at a probability level of $p < 0.05$ was performed to determine
313 whether there were significant differences between analysed films with the null
314 hypothesis being that the analysed samples were the same. When an
315 experimental value of t was greater than the t table value, the difference between
316 samples was significant and the null hypothesis was rejected. All results are
317 expressed as (mean \pm standard deviation) with the exception of the TGA and
318 DSC results where only one measurement of each sample was obtained.

319

320 **3 Results and Discussion**

321 **3.1 Nanoparticle Characterization**

322 The small size of nanoparticles is the key characteristic property that
323 influences their unique properties such as active agent delivery and release
324 (Gaumet, Vargas, Gurny & Delie, 2008; Roussaki et al., 2014). The high surface
325 area-to-volume ratio of smaller nanoparticles facilitates a rapid active agent
326 release and conversely, a greater amount of active agent can be encapsulated
327 in larger nanoparticles resulting in slower release (Singh & Lillard, 2009). In the
328 current investigation, two sizes of nanoparticles were synthesised with particle
329 sizes of ca. 47 and 117 nm respectively. The incorporation of different sizes of
330 nanoparticles can potentially impart a controlled active agent release capacity
331 that is vital for enhancing the AO effect, extending the lifetime of the active

332 material, and prolonging the shelf-life of food products. One major problem that
333 is often encountered in active packaging is the short effective lifetime of many
334 active agents due to their rapid and complete release over a short period of time.
335 However, when the AOs incorporated into the polymer act as radical scavengers,
336 their release is not necessary to achieve an AO effect, as has been demonstrated
337 in several publications (Carrizo et al., 2016). This behaviour opens the door to
338 the possibility of encapsulating AOs to protect them in extrusion processes.
339 Interestingly, the size of both types of unloaded nanoparticles was ca. 244 nm
340 suggesting that the addition of GTE extract further modified the size of the PLA
341 nanoparticles. The smaller size of the GTE-loaded nanoparticles may be due to
342 the presence of the hydroxyl groups in the GTE catechins. These hydroxyl groups
343 can interact with the carboxyl groups of PLA via hydrogen bonding, thus resulting
344 in smaller sized nanoparticles (Arrieta, López, López, Kenny & Peponi, 2016).
345 The size distribution of each of the different types of nanoparticles that were
346 synthesized was calculated from measurements of the scattered light intensity
347 produced by the particles. In all cases, monomodal size distributions were
348 obtained and the width of the size distribution for the small nanoparticles (NP47)
349 was approximately 100 nm whereas that of the larger nanoparticles (NP117) and
350 blank nanoparticles (BK244) was approximately 200 nm.

351 Zeta potential is a measure of the magnitude of the electrostatic or charge
352 repulsion/attraction between particles and is an important parameter that is
353 related to nanoparticle stability or aggregation in solution (Patra & Baek, 2014).
354 The PLA nanoparticles loaded with GTE exhibited negative zeta potentials that
355 were -27 mV and -32 mV for NP47 and NP117 samples respectively. The results
356 suggest that there is strong electrostatic repulsion preventing aggregation of the

357 GTE-loaded nanoparticles (Pool et al., 2012). The charge of the unloaded
358 nanoparticles was only slightly negative (ca. -1 mV) suggesting that the
359 incorporation of GTE affected not only the size but also the surface
360 characteristics. The polydispersity index (PDI) was also determined with values
361 between 0.21 and 0.27 indicating relatively homogeneous samples with
362 moderate PDIs. In this case, the distribution of nanoparticles is neither extremely
363 polydisperse, nor broad, nor in any sense narrow (Roussaki et al., 2014). A
364 summary of the size, zeta potential and PDI results is presented in Table 1.

365

366 Table 1. Size, distribution and zeta potential of unloaded and GTE-loaded
367 nanoparticles. All measurements were performed in triplicate.

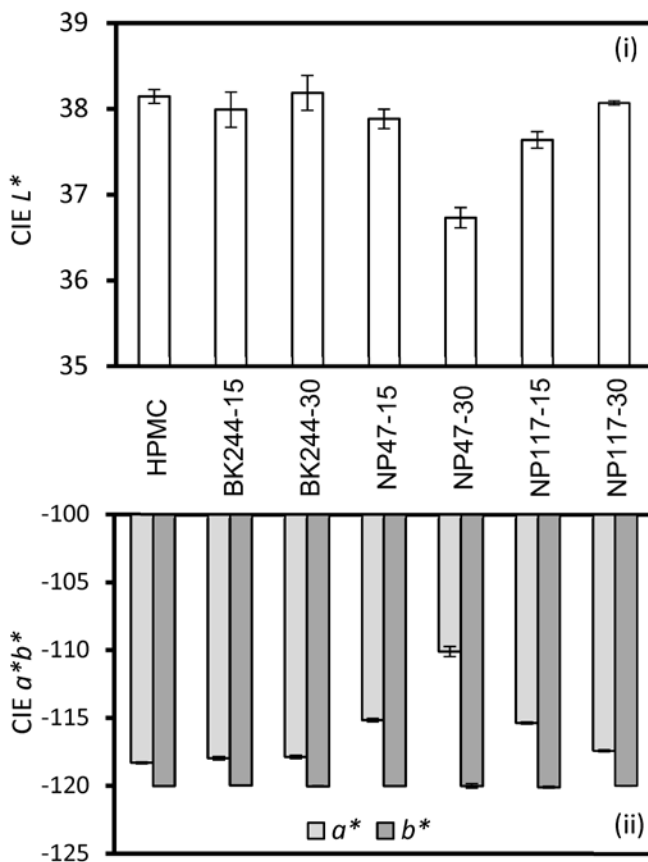
Sample	Particle size/nm	Zeta potential/eV	PDI
BK244	244.4 ± 4.5	-1.38 ± 0.01	0.23 ± 0.02
NP47	47.0 ± 0.5	-27.33 ± 0.15	0.25 ± 0.01
NP117	117.4 ± 0.4	-32.47 ± 0.12	0.27 ± 0.02

368

369 3.2 Film Colour Analysis

370 The CIE $L^*a^*b^*$ parameters for all HPMC samples are presented in Figure 1.
371 Analysis of L^* values representing the whiteness of the film samples suggests no
372 significant difference was obtained in the case of neat HPMC samples and both
373 types of HPMC mixed with unloaded PLA nanoparticles. In the case of the HPMC
374 samples mixed with GTE-loaded nanoparticles and neat nanoparticles at different
375 concentrations, the addition of 30% w/w NP47 particles to the HPMC matrix
376 clearly darkened the films. Since smaller nanoparticles have a larger surface area
377 than larger ones, the active ingredient, in this case dark green GTE, will be sorbed

378 in a greater amount on the shell of the smaller nanoparticles. As a consequence,
379 this may result in the observed decrease in the white coloration of the HPMC film.
380 The addition of other types and concentrations of GTE-loaded nanoparticles had
381 no significant influence on the film whiteness. The addition of all sizes,
382 concentrations, and GTE loadings of PLA nanoparticles into the HPMC films
383 significantly changed the a^* parameter, increasing the redness. The results
384 suggest that this change is primarily influenced by the addition of the
385 nanoparticles rather than the addition of the active agent. Conversely, the b^*
386 parameter remained relatively unchanged with the addition of any type of
387 nanoparticle at the various concentrations that were investigated. Overall, the
388 most significant colour difference was that observed between the neat HPMC film
389 and the sample containing 30% w/w NP47 nanoparticles.



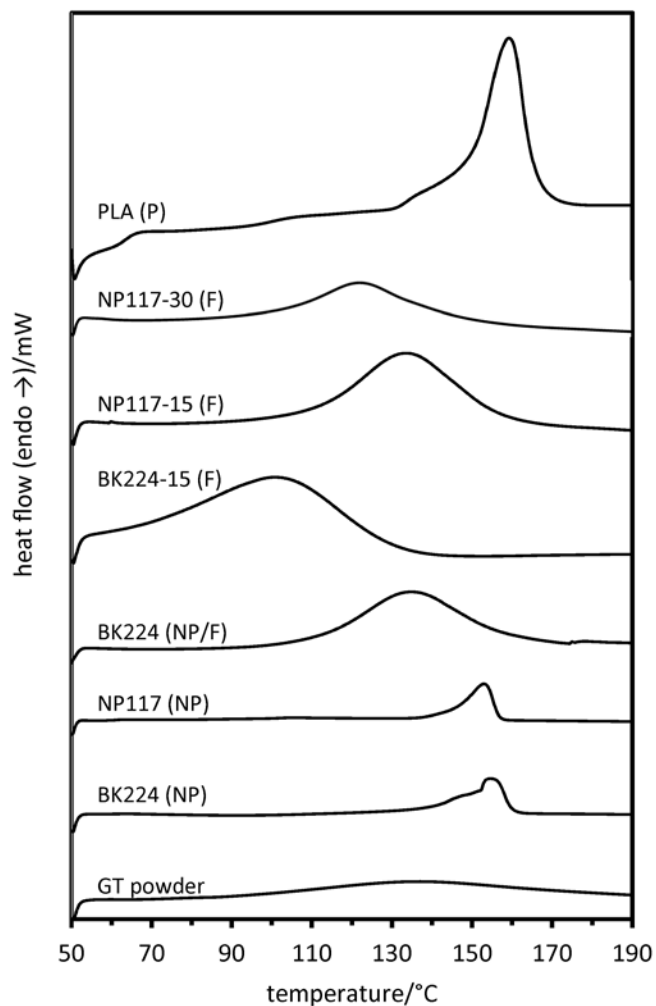
390
391
392
393
394 Figure 1. Results of CIE $L^*a^*b^*$ values for HPMC film samples. All
395 measurements were performed in triplicate.
396

397 **3.3 Thermal Properties**

398 Differential scanning calorimetric analysis was used to determine the
399 thermal properties of the nanoparticles and films with examples of the obtained
400 DSC thermograms presented in Figure 2. The resulting melting points, melting
401 enthalpies and crystallinities are presented in Table 2. The results show that the
402 samples of PLA nanoparticles (both unloaded and loaded) have melting points
403 between 148°C and 153°C compared with the pure PLA pellets that melted at
404 157°C. The result for the pure PLA polymer is slightly higher than that previously
405 reported for the same batch of material (Tawakkal, Cran & Bigger, 2014) and this
406 may be due to differences in the dryness of the sample at the time of recording

407 the DSC thermogram. The melting of bulk materials is generally different to that
408 which occurs at a nanoscale and this occurs mainly as a result of the ratio of
409 surface atoms to the total atoms in the material. Therefore, in the case of PLA, a
410 clear difference in the melting point is observed between the PLA pellet and the
411 nanoscale PLA (Jha, Gupta & Talati, 2008; Kim & Lee, 2009; Takagi, 1954). The
412 same effect was observed in the case of the calculated melting enthalpies and
413 crystallinity results.

414 The polymer crystallinity expressed as ΔH_m was obtained from DSC
415 thermograms in reference to the melting enthalpy of 100% crystalline polymer
416 matrix which is 93 J g⁻¹ for PLA (Battegazzore, Bocchini & Frache, 2011). The
417 addition of nanoparticles to the HPMC matrix decreased the melting temperature
418 of the materials. Conversely, the melting enthalpies of each of the HPMC films
419 containing PLA nanoparticles were always higher than that of the neat HPMC
420 film. It was observed that the melting enthalpy of HPMC films prepared with 30%
421 w/w of any type of nanoparticle solution was lower than that of HPMC films
422 containing 15% w/w of nanoparticle solution. Pure HPMC is a totally amorphous
423 polymer that does not display endothermic peaks upon melting (data not shown).
424 The DSC thermogram of the neat green tea powder is also shown for comparison
425 and exhibits a broad melting peak at ca. 132°C. The neat green tea powder is
426 comprised of a complex mixture of many different components including
427 carbohydrates (cellulose), lipids, trace minerals, vitamins and polyphenols (Chu
428 & Juneja, 1997).



429
430 Figure 2. DSC thermograms of green tea powder, PLA pellet, nanoparticles and
431 HPMC films. Letters in brackets refer to: (P) pellet; (NP) nanoparticles; and (F)
432 film. Single experiments were performed.
433

434 Table 2. Peak melting points, melting enthalpies and crystallinity of
 435 nanoparticles and HPMC films. Single experiments were performed.

Sample	$T_m /^\circ\text{C}$	$\Delta H_m/\text{J g}^{-1}$	$X_c\%$
GT powder	132	331	-
PLA pellet	157	437	4.7
BK244	153	73	0.8
NP47	148	68	0.7
NP117	152	54	0.6
HPMC	132	230	-
BK244-15	97	376	-
BK244-30	100	295	-
NP47-15	129	272	-
NP47-30	93	249	-
NP117-15	130	268	-
NP117-30	120	242	-

436

437 **3.4 Structural Properties**

438 The structure of the PLA nanoparticles and HPMC film samples were
 439 elucidated by ATR FTIR analyses and the spectra of selected materials are
 440 presented in the supplement. The spectrum of the neat PLA nanoparticles
 441 corresponds to the spectrum of pure PLA characterised with a summary of the
 442 key peaks presented in Table 3. The absence of a broad peak between 3700-
 443 3000 cm^{-1} confirms the absence of moisture in the dried PLA which has been
 444 shown previously for the same batch of PLA (Tawakkal, Cran & Bigger, 2016)
 445 and in other PLA systems ((Xiao et al., 2012)). In the case of the PLA

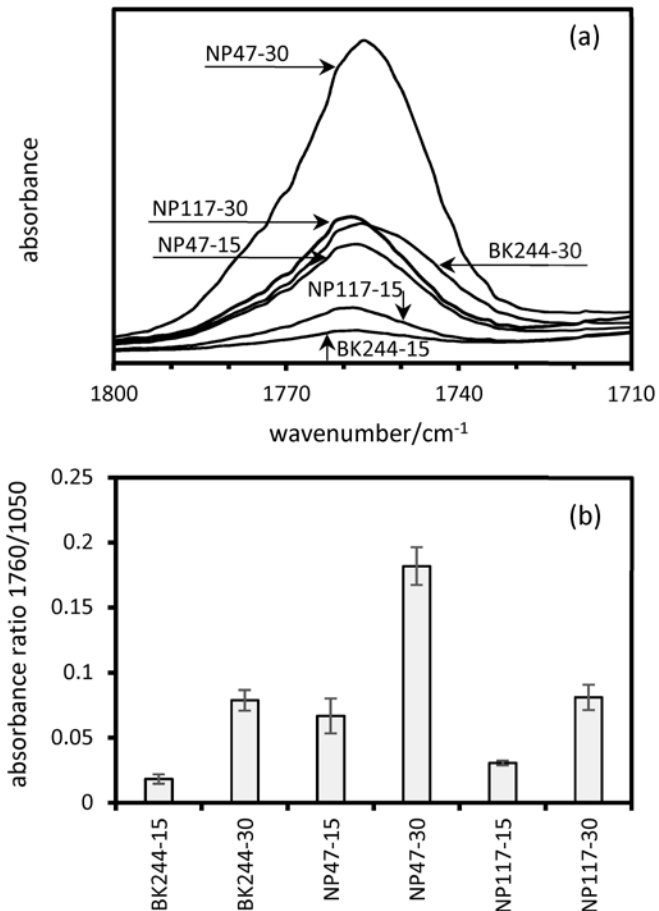
446 nanoparticles loaded with GTE, the spectra are very similar to that of the
447 unloaded PLA nanoparticles with some changes observed in the peak at
448 1640 cm^{-1} which undergoes a bathochromic shift in the case of the loaded PLA
449 nanoparticles. This peak corresponds to C=C and/or C-N stretches in the GTE
450 (Senthilkumar & Sivakumar, 2014) and the shift may indicate some interaction
451 between the GTE and the PLA.

452 In the case of the HPMC films, the various characteristic peaks associated
453 with this material are also presented in Table 3. When combined with the PLA
454 nanoparticles, changes in peak intensities were observed between samples with
455 different concentrations of loaded nanoparticles. In general, the higher loadings
456 of nanoparticles resulted in lower HPMC peak intensities as expected due to the
457 reduced HPMC content. An exception was observed in case of the peak at
458 1760 cm^{-1} which can be attributed to the carbonyl groups from PLA which are
459 introduced into the HPMC matrix (Okunlola, 2015). This peak is shown in Figure
460 3(a) for the various film samples where lower peak intensities are observed for
461 the films containing 15% w/w PLA nanoparticles as compared with the same films
462 containing 30% w/w PLA nanoparticles. When these peaks are normalized to a
463 characteristic HPMC peak (1050 cm^{-1}) as shown in Figure 3(b), the most intense
464 peak is produced by the sample containing the smaller (47 nm) GTE-loaded
465 nanoparticles at the highest loading of these in the polymer. This, in turn,
466 suggests the greatest interaction between the nanoparticles and the HPMC
467 polymer matrix occurs in that sample.

468
469

470 Table 3. Summary of key ATR-FTIR spectral peaks of PLA nanoparticles and
471 HPMC films.

Wave-number(s)/cm ⁻¹	PLA functional groups	HPMC functional groups	References
~3400	OH stretching (typically not seen in dried PLA)	OH stretching	Sekharan, Palanichamy, Tamilvanan, Shanmuganathan and Thirupathi (2011), Gustafsson, Nyström, Lennholm, Bonferoni and Caramella (2003)
3000-2800	C-H stretching	C-H symmetric and asymmetric valence vibrations from CH ₃	Lopes, Jardini and Filho (2014) Sekharan, Palanichamy, Tamilvanan, Shanmuganathan and Thirupathi (2011)
1760-1750	C=O stretching	C=O stretching or deformation, O-CO stretching	Okunlola (2015)
1640-1650	C=C and/or C-N stretches in GTE, absorbed water		Senthilkumar and Sivakumar (2014), Sakata, Shiraishi and Otsuka (2006)
1489, 1452, 1412	-C-H bending		Sakata, Shiraishi and Otsuka (2006)
1383		CH ₃ symmetric bending, CH bending, or C-CH ₃ stretching	Kang, Hsu, Stidham, Smith, Leugers and Yang (2001)
1359		C-COO stretching, O-CH stretching, O-CO stretching, or C=O in-plane bending	Kang, Hsu, Stidham, Smith, Leugers and Yang (2001)
1337, 1315	-C-H bending		Sakata, Shiraishi and Otsuka (2006)
1190-1180	C-O-C and C-O stretching alcohol	C-COO stretching, O-CH stretching, CH ₃ rocking, or CH bending	Kang, Hsu, Stidham, Smith, Leugers and Yang (2001), Sakata, Shiraishi and Otsuka (2006)
1130		CH bending or O-CH stretching	Kang, Hsu, Stidham, Smith, Leugers and Yang (2001)
1080		C-CH ₃ stretching, CH ₃ rocking, or skeletal CCO bending	Kang, Hsu, Stidham, Smith, Leugers and Yang (2001)
1040-1060	C-O-C and C-O stretching alcohol	CH ₃ rocking, CH bending, or C-COO stretching	Kang, Hsu, Stidham, Smith, Leugers and Yang (2001), Sakata, Shiraishi and Otsuka (2006)
948	C-O-C and C-O stretching alcohol		Sakata, Shiraishi and Otsuka (2006)
871		C-COO stretching, C-CH ₃ stretching, O-CO stretching, skeletal COC bending, or C=O deformation	Kang, Hsu, Stidham, Smith, Leugers and Yang (2001)
760		C-CH ₃ stretching, skeletal CCO bending, C=O in-plane bending, or C=O out-of-plane bending	Kang, Hsu, Stidham, Smith, Leugers and Yang (2001)



473

474 Figure 3. Infrared peaks of HPMC film samples between 1800-1710 cm⁻¹ (a)
 475 and absorbance ratios of peaks at 1760 to 1050 cm⁻¹ (b). All measurements
 476 were performed in triplicate.

477

478 **3.5 Nanoparticle and Film Imaging**

479 The SEM micrographs of selected loaded and unloaded nanoparticles and HPMC
 480 films are presented in Figure 4. It can be observed that the neat nanoparticles
 481 are significantly larger than the GTE-loaded nanoparticles and this is consistent
 482 with results obtained using the light scattering particle sizing instrument. It is
 483 interesting to note that the neat PLA appears to form not only nanoparticles but
 484 also nanofibers whereas the GTE-loaded PLA nanoparticles are primarily
 485 spherical and much smaller. Although image analysis of the HPMC films was
 486 challenged by some damage to the films caused by the SEM beam, the images

487 of neat HPMC film and those containing the different types and concentrations of
488 nanoparticles demonstrated mainly smooth, homogeneous surfaces as shown in
489 images (c) to (g). It can therefore be suggested that the nanoparticles
490 incorporated into the HPMC matrix remained separate and this is in accordance
491 with the strong negative charge of the particles identified by the zeta potential
492 measurements.

493

494

495

496

497

498

499

500

501

502

503

504

505

506

507

508

509

510

511

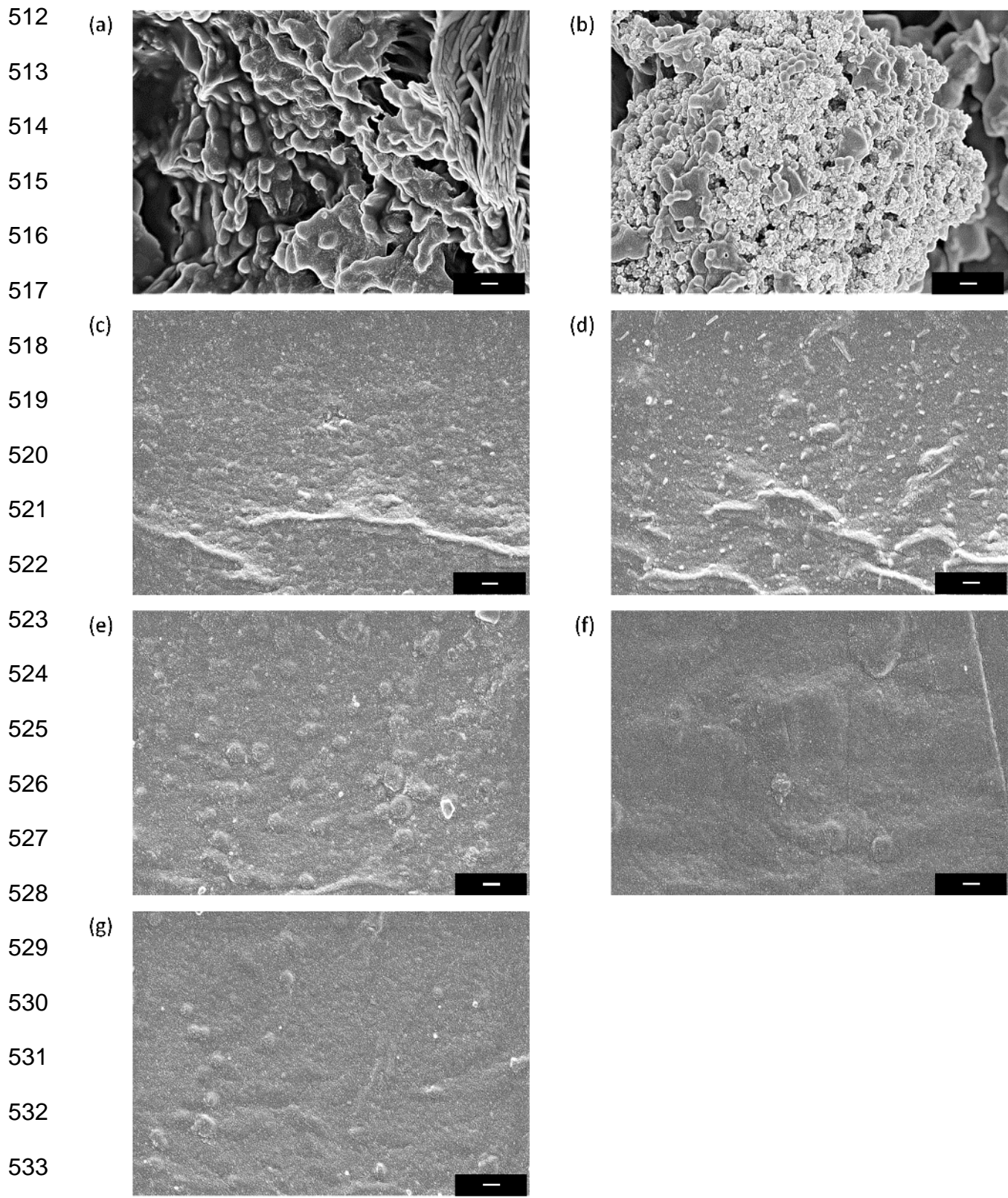


Figure 4. SEM micrographs of: (a) neat nanoparticles; (b) loaded NP2 nanoparticles; (c) neat HPMC film; (d) HPMC film with 30% neat nanoparticle solution; (e) HPMC film with 60% nanoparticle solution; (f) HPMC film with 30% NP2 solution and (g); HPMC film with 60% NP2 solution. Scale bars are 200 nm.

540 **3.6 Green Tea Migration and Antioxidant Capacity**

541 In general, the timely migration of encapsulated active compounds is critical
542 in providing sustained and adequate AO activity. The results of migration testing
543 of the GTE from the PLA nanoparticles incorporated in the HPMC film matrix are
544 presented in Table 4. The data show that there was no significant difference
545 between the samples for the migration test performed at 20°C. It can be clearly
546 seen that a significantly higher extent of GTE migration occurred at 40°C,
547 particularly in the case of the smaller nanoparticles (NP47). The latter suggests
548 that the small nanoparticles impart a greater active agent release due to their
549 high surface area-to-volume ratio. A comparison between the same types of
550 nanoparticles at different loadings reveals that more active compound was
551 liberated in the case of the higher nanoparticle loading as expected.

552 The AO capacities of the solutions obtained from the migration tests are
553 also presented in Table 4. The absorbance of DPPH in the presence of the control
554 samples was the same as those in methanol so no AO capacity was observed in
555 the case of the unloaded nanoparticle film samples. As expected, the samples
556 investigated in the migration tests performed at 40°C and those with higher
557 nanoparticle loadings were all characterised by higher CAOX values of the
558 solutions. Moreover, the smaller (47 nm) nanoparticles incorporated into the
559 HPMC matrix (NP47) produced higher CAOX values than those films containing
560 the larger (117 nm) particles. A recent study of the AO capacity of crude green
561 tea extract reported an IC₅₀ value of ca. 250 µg g⁻¹ (Kusmita, Puspitaningrum &
562 Limantara, 2015). Clearly, it is difficult to make comparisons between studies
563 given the high variability in the composition of GTEs, the method of extraction,
564 and the method of AO capacity testing. However, the result of Kusmita,

565 Puspitaningrum and Limantara (2015) is significantly numerically higher than the
566 CAOX values found in the present study for the NP47-30 film at both
567 temperatures and that of the NP47-15 film at 40°C suggesting that the active
568 agent encapsulated in PLA nanoparticles has an apparently greater AO capacity.

569

570 Table 4. Results of migration testing after 10 days and subsequent antioxidant
571 capacity of migration solution. All measurements were performed in triplicate.

Sample	GTE Liberation (%)		IC ₅₀ /μg g ⁻¹	
	20°C	40°C	20°C	40°C
NP47-15	35 ± 13	51 ± 10	249 ± 36	224 ± 8
NP47-30	36 ± 14	84 ± 16	211 ± 11	203 ± 2
NP117-15	38 ± 4	39 ± 13	373 ± 12	361 ± 6
NP117-30	39 ± 1	56 ± 3	335 ± 31	308 ± 9

572

573 Although the application of PLA nanoparticles has been previously reported
574 in the area of controlled drug delivery systems (Lee, Yun & Park, 2016), there are
575 very few commercially available active packaging materials incorporating PLA
576 nanoparticles that are specifically designed to extend the shelf-life of food
577 products (Kuorwel, Cran, Orbell, Buddhadasa & Bigger, 2015). Moreover, there
578 are very few reports of controlled release AOs encapsulated in PLA nanoparticles
579 used in food packaging applications. However, various challenges in the
580 production of PLA nanoparticles have been reported in the scientific literature.
581 One of them is the low reproducibility between batches and the heterogeneity in
582 shape and size of nanoparticles (Kumar, Shafiq & Malhotra, 2012; Mitragotri,
583 Burke & Langer, 2014; Yun, Lee & Park, 2015). In the present study, the

584 systematic application of the MODDE software for the optimisation of the
585 synthesis, highly reproducible, homogeneous shape and size nanoparticles were
586 obtained. Moreover, the physico-chemical characterization of PLA nanoparticles
587 in the recent literature, particularly those loaded with active agents, is relatively
588 limited (Lee, Yun & Park, 2016). The present study, is an important step in
589 ascertaining some of these critical properties.

590

591 **4 Conclusions**

592 A new active bio-based material utilizing HPMC incorporated with GTE-
593 loaded PLA nanoparticles was successfully developed. The optimization of the
594 synthesis of PLA nanoparticles resulted in the production of GTE-loaded
595 nanoparticles that were spherical and uniform in size. When incorporated into
596 HPMC film, a slight change in film redness was observed with both loaded and
597 unloaded PLA nanoparticles. Thermal and infrared analyses suggested some
598 molecular interactions between PLA and GTE as well as the PLA and HPMC
599 matrix. Migration and AO capacity testing confirmed that higher AO capacity was
600 observed when the GTE was liberated at a higher temperature as expected and
601 the release was generally dependent on the size of the nanoparticles. The results
602 of the present study suggest that HPMC films containing GTE-loaded PLA
603 nanoparticles could be used for packaging applications aimed at extending the
604 shelf life of food products with high fat contents. Furthermore, such active HPMC
605 films could be used as an inner layer in multilayer packaging that could further
606 extend the potential applications.

607

608

609 **5 Acknowledgment**

610 M. Wrona acknowledges the FPU grant (reference number AP2012-2716)
611 received from the MEC, Ministerio de Educación, Cultura y Deporte, Spain.
612 Thanks are given to Project AGL2012-37886 from MINECO (Spain) and FEDER
613 funds for financial support.

614

615 **6 References**

- 616 Akhtar, M. J., Jacquot, M., Arab-Tehrany, E., Gaiani, C., Linder, M., & Desobry,
617 S. (2010). Control of salmon oil photo-oxidation during storage in HPMC
618 packaging film: Influence of film colour. *Food Chemistry*, 120(2), 395-401.
- 619 Akhtar, M. J., Jacquot, M., Jasniewski, J., Jacquot, C., Imran, M., Jamshidian,
620 M., Paris, C., & Desobry, S. (2012). Antioxidant capacity and light-aging study of
621 HPMC films functionalized with natural plant extract. *Carbohydrate Polymers*,
622 89(4), 1150-1158.
- 623 Armentano, I., Bitinis, N., Fortunati, E., Mattioli, S., Rescignano, N., Verdejo, R.,
624 Lopez-Manchado, M. A., & Kenny, J. M. (2013). Multifunctional nanostructured
625 PLA materials for packaging and tissue engineering. *Progress in Polymer
626 Science*, 38(10–11), 1720-1747.
- 627 Arrieta, M. P., López, J., López, D., Kenny, J. M., & Peponi, L. (2016). Effect of
628 chitosan and catechin addition on the structural, thermal, mechanical and
629 disintegration properties of plasticized electrospun PLA-PHB biocomposites.
630 *Polymer Degradation and Stability*, *in press*.
- 631 Auras, R., Harte, B., & Selke, S. (2004). An overview of polylactides as packaging
632 materials. *Macromolecular Bioscience*, 4(9), 835-864.
- 633 Bang, G., & Kim, S. W. (2012). Biodegradable poly(lactic acid)-based hybrid
634 coating materials for food packaging films with gas barrier properties. *Journal of
635 Industrial and Engineering Chemistry*, 18(3), 1063-1068.

- 636 Battegazzore, D., Bocchini, S., & Frache, A. (2011). Crystallization kinetics of
637 poly(lactic acid)-talc composites. *eXPRESS Polymer Letters*, 5(10), 849-858.
- 638 Bilbao-Sainz, C., Avena-Bustillos, R. J., Wood, D. F., Williams, T. G., & McHugh,
639 T. H. (2010). Composite edible films based on hydroxypropyl methylcellulose
640 reinforced with microcrystalline cellulose nanoparticles. *Journal of Agricultural
641 and Food Chemistry*, 58(6), 3753-3760.
- 642 Bolumar, T., Andersen, M. L., & Orlien, V. (2011). Antioxidant active packaging
643 for chicken meat processed by high pressure treatment. *Food Chemistry*, 129(4),
644 1406-1412.
- 645 Brindle, L. P., & Krochta, J. M. (2008). Physical properties of whey protein-
646 hydroxypropylmethylcellulose blend edible films. *Journal of Food Science*, 73(9),
647 E446-E454.
- 648 Camo, J., Lorés, A., Djennane, D., Beltrán, J. A., & Roncalés, P. (2011). Display
649 life of beef packaged with an antioxidant active film as a function of the
650 concentration of oregano extract. *Meat Science*, 88(1), 174-178.
- 651 Carrizo, D., Gullo, G., Bosetti, O., & Nerín, C. (2014). Development of an active
652 food packaging system with antioxidant properties based on green tea extract.
653 *Food Additives and Contaminants: Part A*, 31(3), 364-373.
- 654 Carrizo, D., Taborda, G., Nerín, C., & Bosetti, O. (2016). Extension of shelf life of
655 two fatty foods using a new antioxidant multilayer packaging containing green tea
656 extract. *Innovative Food Science & Emerging Technologies*, 33, 534–541.
- 657 Chu, D.-C., & Juneja, L. R. (1997). General Chemical Composition of Green Tea
658 and its Infusion. In T. Yamamoto, L. R. Juneja, D.-C. Chu & M. Kim (Eds.).
659 *Chemistry and Applications of Green Tea* (Vol. 2, pp. 13-22): CRC Press LLC.
- 660 Cirillo, G., Spizzirri, U. G., & Iemma, F. (2015). *Functional Polymers in Food
661 Science: From Technology to Biology, Volume 1: Food Packaging*. Wiley.

- 662 Colon, M., & Nerin, C. (2012). Role of Catechins in the Antioxidant Capacity of
663 an Active Film Containing Green Tea, Green Coffee, and Grapefruit Extracts.
664 *Journal of Agricultural and Food Chemistry*, 60(39), 9842-9849.
- 665 Cusheen, M., Kerry, J., Morris, M., Cruz-Romero, M., & Cummins, E. (2012).
666 Nanotechnologies in the food industry – Recent developments, risks and
667 regulation. *Trends in Food Science and Technology*, 24(1), 30-46.
- 668 de Moura, M. R., Aouada, F. A., Avena-Bustillos, R. J., McHugh, T. H., Krochta,
669 J. M., & Mattoso, L. H. C. (2009). Improved barrier and mechanical properties of
670 novel hydroxypropyl methylcellulose edible films with chitosan/tripolyphosphate
671 nanoparticles. *Journal of Food Engineering*, 92(4), 448-453.
- 672 de Moura, M. R., Avena-Bustillos, R. J., McHugh, T. H., Krochta, J. M., & Mattoso,
673 L. H. C. (2008). Properties of novel hydroxypropyl methylcellulose films
674 containing chitosan nanoparticles. *Journal of Food Science*, 73(7), N31-N37.
- 675 DeGruson, M. L. (2016). Biobased Packaging. *Reference Module in Food
676 Science*: Elsevier.
- 677 Del Nobile, M. A., Conte, A., Buonocore, G. G., Incoronato, A. L., Massaro, A., &
678 Panza, O. (2009). Active packaging by extrusion processing of recyclable and
679 biodegradable polymers. *Journal of Food Engineering*, 93(1), 1-6.
- 680 Ding, C., Zhang, M., & Li, G. (2015). Preparation and characterization of
681 collagen/hydroxypropyl methylcellulose (HPMC) blend film. *Carbohydrate
682 Polymers*, 119, 194-201.
- 683 Dow Chemical Company. (2002). METHOCEL Cellulose Ethers Technical
684 Handbook, available from:
685 <http://www.dow.com/webapps/lit/litorder.asp?filepath=methocel/pdfs/noreg/192-01062.pdf>.
- 687 Duncan, T. V. (2011). Applications of nanotechnology in food packaging and food
688 safety: Barrier materials, antimicrobials and sensors. *Journal of Colloid and
689 Interface Science*, 363(1), 1-24.

- 690 European Commission. (2011). Regulation (EU) No 10/2011 of 14 January 2011
691 on plastic materials and articles intended to come into contact with food. (Vol.
692 10/2011): Official Journal of the European Union.
- 693 Fabra, M. J., López-Rubio, A., & Lagaron, J. M. (2014). Biopolymers for food
694 packaging applications. In M. R. Aguilar & J. S. Román (Eds.). *Smart Polymers*
695 and their Applications (pp. 476-509): Woodhead Publishing.
- 696 Falowo, A. B., Fayemi, P. O., & Muchenje, V. (2014). Natural antioxidants against
697 lipid–protein oxidative deterioration in meat and meat products: A review. *Food*
698 *Research International*, 64, 171-181.
- 699 Fang, Z., & Bhandari, B. (2010). Encapsulation of polyphenols – a review. *Trends*
700 *in Food Science and Technology*, 21(10), 510-523.
- 701 Frankel, E. N., Huang, S.-W., & Aeschbach, R. (1997). Antioxidant Activity of
702 Green Teas in Different Lipid Systems. *Journal of the American Oil Chemists' Society*, 74(10), 1309-1315.
- 704 Friskin, B. J. (2001). Revisiting the Method of Cumulants for the Analysis of
705 Dynamic Light-Scattering Data. *Applied Optics*, 40(24), 4087-4091.
- 706 Gadkari, P. V., & Balaraman, M. (2015). Catechins: Sources, extraction and
707 encapsulation: A review. *Food and Bioproducts Processing*, 93, 122-138.
- 708 Gao, H., Jones, M.-C., Chen, J., Liang, Y., Prud'homme, R. E., & Leroux, J.-C.
709 (2008). Hydrophilic Nanoreservoirs Embedded into Polymeric
710 Micro/Nanoparticles: An Approach To Compatibilize Polar Molecules with
711 Hydrophobic Matrixes. *Chemistry of Materials*, 20(13), 4191-4193.
- 712 Gaumet, M., Vargas, A., Gurny, R., & Delie, F. (2008). Nanoparticles for drug
713 delivery: The need for precision in reporting particle size parameters. *European*
714 *Journal of Pharmaceutics and Biopharmaceutics*, 69(1), 1-9.
- 715 Gustafsson, C., Nyström, C., Lennholm, H., Bonferoni, M. C., & Caramella, C. M.
716 (2003). Characteristics of hydroxypropyl methylcellulose influencing compatibility

- 717 and prediction of particle and tablet properties by infrared spectroscopy. *Journal*
718 *of Pharmaceutical Sciences*, 92(3), 494-504.
- 719 Hirsjärvi, S. (2008). Preparation and Characterization of Poly(Lactic Acid)
720 Nanoparticles for Pharmaceutical Use. MSc dissertation. Division of
721 Pharmaceutical Technology, Faculty of Pharmacy: University of Helsinki.
- 722 Imran, M., Klouj, A., Revol-Junelles, A.-M., & Desobry, S. (2014). Controlled
723 release of nisin from HPMC, sodium caseinate, poly-lactic acid and chitosan for
724 active packaging applications. *Journal of Food Engineering*, 143, 178-185.
- 725 Jha, P. K., Gupta, S. K., & Talati, M. (2008). Shape and Size Dependent Melting
726 Point Temperature of Nanoparticles. *Materials Science Forum*, 570, 132-137.
- 727 Kang, S., Hsu, S. L., Stidham, H. D., Smith, P. B., Leugers, M. A., & Yang, X.
728 (2001). A Spectroscopic Analysis of Poly(lactic acid) Structure. *Macromolecules*,
729 34(13), 4542-4548.
- 730 Kim, E.-H., & Lee, B.-J. (2009). Size dependency of melting point of crystalline
731 nano particles and nano wires: A thermodynamic modeling. *Metals and Materials*
732 *International*, 15(4), 531-537.
- 733 Kumar, G., Shafiq, N., & Malhotra, S. (2012). Drug-Loaded PLGA Nanoparticles
734 for Oral Administration: Fundamental Issues and Challenges Ahead. *Critical*
735 *Reviews™ in Therapeutic Drug Carrier Systems*, 29(2), 149-182.
- 736 Kuorwel, K. K., Cran, M. J., Orbell, J. D., Buddhadasa, S., & Bigger, S. W. (2015).
737 Review of Mechanical Properties, Migration, and Potential Applications in Active
738 Food Packaging Systems Containing Nanoclays and Nanosilver. *Comprehensive*
739 *Reviews in Food Science and Food Safety*, 14(4), 411-430.
- 740 Kusmita, L., Puspitaningrum, I., & Limantara, L. (2015). Identification, Isolation
741 and Antioxidant Activity of Pheophytin from Green Tea (*Camellia Sinensis* (L.)
742 Kuntze). *Procedia Chemistry*, 14, 232-238.
- 743 Lee, B. K., Yun, Y., & Park, K. (2016). PLA micro- and nano-particles. *Advanced*
744 *Drug Delivery Reviews*, *in press*.

- 745 Lim, J., Yeap, S. P., Che, H. X., & Low, S. C. (2013). Characterization of magnetic
746 nanoparticle by dynamic light scattering. *Nanoscale Research Letters*, 8, 381.
- 747 Llana-Ruiz-Cabello, M., Pichardo, S., Jimenez-Morillo, N. T., Bermudez, J. M.,
748 Aucejo, S., Gonzalez-Vila, F. J., Camean, A. M., & Gonzalez-Perez, J. A. (2015).
749 Molecular characterization of a bio-based active packaging containing *Origanum*
750 *vulgare* L. essential oil using pyrolysis gas chromatography/mass spectrometry
751 (Py-GC/MS). *Journal of the Science of Food and Agriculture*, early view.
- 752 Lopes, M. S., Jardini, A. L., & Filho, R. M. (2014). Synthesis and
753 Characterizations of Poly (Lactic Acid) by Ring-Opening Polymerization for
754 Biomedical Applications. *Chemical Engineering Transactions*, 38, 331-336.
- 755 López-de-Dicastillo, C., Gómez-Estaca, J., Catalá, R., Gavara, R., & Hernández-
756 Muñoz, P. (2012). Active antioxidant packaging films: Development and effect on
757 lipid stability of brined sardines. *Food Chemistry*, 131(4), 1376-1384.
- 758 Ma, P.-C., Siddiqui, N. A., Marom, G., & Kim, J.-K. (2010). Dispersion and
759 functionalization of carbon nanotubes for polymer-based nanocomposites: A
760 review. *Composites Part A: Applied Science and Manufacturing*, 41(10), 1345-
761 1367.
- 762 Min, B., & Ahn, D. U. (2005). Mechanism of Lipid Peroxidation in Meat and Meat
763 Products -A Review. *Food Science and Biotechnology*, 14(1), 152-163.
- 764 Mitragotri, S., Burke, P. A., & Langer, R. (2014). Overcoming the challenges in
765 administering biopharmaceuticals: formulation and delivery strategies. *Nature*
766 *Reviews Drug Discovery*, 13(9), 655-672.
- 767 Okunlola, A. (2015). Design of bilayer tablets using modified *Dioscorea* starches
768 as novel excipients for immediate and sustained release of aceclofenac sodium.
769 *Frontiers in Pharmacology*, 5, Article 294.
- 770 Patra, J. K., & Baek, K.-H. (2014). Green Nanobiotechnology: Factors Affecting
771 Synthesis and Characterization Techniques. *Journal of Nanomaterials*, art
772 417305, 12.

- 773 Paul, D. R., & Robeson, L. M. (2008). Polymer nanotechnology:
774 Nanocomposites. *Polymer*, 49(15), 3187-3204.
- 775 Pool, H., Quintanar, D., Figueroa, J. d. D., Marinho Mano, C., Bechara, J. E. H.,
776 Godínez, L. A., & Mendoza, S. (2012). Antioxidant Effects of Quercetin and
777 Catechin Encapsulated into PLGA Nanoparticles. *Journal of Nanomaterials*,
778 2012, 12.
- 779 Pyrzynska, K., & Pękal, A. (2013). Application of free radical
780 diphenylpicrylhydrazyl (DPPH) to estimate the antioxidant capacity of food
781 samples. *Analytical Methods*, 5(17), 4288.
- 782 Rancan, F., Papakostas, D., Hadam, S., Hackbarth, S., Delair, T., Primard, C.,
783 Verrier, B., Sterry, W., Blume-Peytavi, U., & Vogt, A. (2009). Investigation of
784 polylactic acid (PLA) nanoparticles as drug delivery systems for local
785 dermatotherapy. *Pharmaceutical Research*, 26(8), 2027-2036.
- 786 Rao, J. P., & Geckeler, K. E. (2011). Polymer nanoparticles: Preparation
787 techniques and size-control parameters. *Progress in Polymer Science*, 36(7),
788 887-913.
- 789 Rhim, J.-W., Park, H.-M., & Ha, C.-S. (2013). Bio-nanocomposites for food
790 packaging applications. *Progress in Polymer Science*, 38(10–11), 1629-1652.
- 791 Roussaki, M., Gaitanarou, A., Diamanti, P. C., Vouyiouka, S., Papaspyrides, C.,
792 Kefalas, P., & Detsi, A. (2014). Encapsulation of the natural antioxidant
793 aureusidin in biodegradable PLA nanoparticles. *Polymer Degradation and
794 Stability*, 108, 182-187.
- 795 Ruan, G., & Feng, S.-S. (2003). Preparation and characterization of poly(lactic
796 acid)-poly(ethylene glycol)-poly(lactic acid) (PLA-PEG-PLA) microspheres for
797 controlled release of paclitaxel. *Biomaterials*, 24(27), 5037-5044.
- 798 Ruffino, F., Torrisi, V., Marletta, G., & Grimaldi, M. G. (2011). Growth morphology
799 of nanoscale sputter-deposited Au films on amorphous soft polymeric substrates.
800 *Applied Physics A*, 103(4), 939-949.

- 801 Sakata, Y., Shiraishi, S., & Otsuka, M. (2006). A novel white film for
802 pharmaceutical coating formed by interaction of calcium lactate pentahydrate
803 with hydroxypropyl methylcellulose. *International Journal of Pharmaceutics*,
804 317(2), 120-126.
- 805 Samsudin, H., Soto-Valdez, H., & Auras, R. (2014). Poly(lactic acid) film
806 incorporated with marigold flower extract (*Tagetes erecta*) intended for fatty-food
807 application. *Food Control*, 46, 55-66.
- 808 Sanchez-Gonzalez, L., Vargas, M., Gonzalez-Martinez, C., Chiralt, A., & Chafer,
809 M. (2009). Characterization of edible films based on
810 hydroxypropylmethylcellulose and tea tree essential oil. *Food Hydrocolloids*,
811 23(8), 2102-2109.
- 812 Sekharan, T. R., Palanichamy, S., Tamilvanan, S., Shanmuganathan, S., &
813 Thirupathi, A. T. (2011). Formulation and Evaluation of Hydroxypropyl
814 Methylcellulose-based Controlled Release Matrix Tablets for Theophylline.
815 *Indian Journal of Pharmaceutical Sciences*, 73(4), 451-456.
- 816 Senanayake, S. P. J. N. (2013). Green tea extract: Chemistry, antioxidant
817 properties and food applications – A review. *Journal of Functional Foods*, 5(4),
818 1529-1541.
- 819 Senthilkumar, S. R., & Sivakumar, T. (2014). Green Tea (*Camellia sinensis*)
820 Mediated Synthesis of Zinc Oxide (ZNO) Nanoparticles and Studies on their
821 Antimicrobial Activities. *International Journal of Pharmacy and Pharmaceutical
822 Sciences*, 6(6), 461-465.
- 823 Silvestre, C., Duraccio, D., & Cimmino, S. (2011). Food packaging based on
824 polymer nanomaterials. *Progress in Polymer Science*, 36(12), 1766-1782.
- 825 Singh, R., & Lillard, J. W. (2009). Nanoparticle-based targeted drug delivery.
826 *Experimental and molecular pathology*, 86(3), 215-223.
- 827 Takagi, M. (1954). Electron-Diffraction Study of Liquid-Solid Transition of Thin
828 Metal Films. *Journal of the Physical Society of Japan*, 9(3), 359-363.

- 829 Tawakkal, I. S. M. A., Cran, M. J., & Bigger, S. W. (2014). Effect of Kenaf Fibre
830 Loading and Thymol Concentration on the Mechanical and Thermal Properties of
831 PLA/Kenaf/Thymol Composites. *Industrial Crops and Products*, 61, 74-83.
- 832 Tawakkal, I. S. M. A., Cran, M. J., & Bigger, S. W. (2016). Interaction and
833 quantification of thymol in active PLA-based materials containing natural fibers.
834 *Journal of Applied Polymer Science*, 133(2), 42160.
- 835 Tawakkal, I. S. M. A., Cran, M. J., Miltz, J., & Bigger, S. W. (2014). A Review of
836 Poly(lactic acid)-Based Materials for Antimicrobial Packaging. *Journal of Food*
837 *Science*, 79(8), R1477-R1490.
- 838 Vrignaud, S., Benoit, J.-P., & Saulnier, P. (2011). Strategies for the
839 nanoencapsulation of hydrophilic molecules in polymer-based nanoparticles.
840 *Biomaterials*, 32(33), 8593-8604.
- 841 Xiao, L., Mai, Y., He, F., Yu, L., Zhang, L., Tang, H., & Yang, G. (2012). Bio-
842 based green composites with high performance from poly(lactic acid) and
843 surface-modified microcrystalline cellulose. *Journal of Materials Chemistry*,
844 22(31), 15732-15739.
- 845 Yam, K. L., & Papadakis, S. E. (2004). A simple digital imaging method for
846 measuring and analyzing color of food surfaces. *Journal of Food Engineering*,
847 61(1), 137-142.
- 848 Yang, H.-J., Lee, J.-H., Won, M., & Song, K. B. (2016). Antioxidant activities of
849 distiller dried grains with solubles as protein films containing tea extracts and their
850 application in the packaging of pork meat. *Food Chemistry*, 196, 174-179.
- 851 Yin, J., Becker, E. M., Andersen, M. L., & Skibsted, L. H. (2012). Green tea extract
852 as food antioxidant. Synergism and antagonism with β -tocopherol in vegetable
853 oils and their colloidal systems. *Food Chemistry*, 135(4), 2195-2202.
- 854 Yun, Y. H., Lee, B. K., & Park, K. (2015). Controlled Drug Delivery: Historical
855 perspective for the next generation. *Journal of Controlled Release*, 219, 2-7.
856